Thermal nucleation and cavitation in ^{3}He and ^{4}He

D. M. Jezek,* M. Guilleumas, M. Pi, and M. Barranco
Departament d'Estructura i Constituents de la Matèria, Facultat de Física, Universitat de Barcelona, E-08028 Barcelona, Spain

J. Navarro
Departament de Física Atòmica, Molecular i Nuclear, and Instituto de Física Corpuscular (Centre Mixt Consejo Superior de Investigaciones Científicas Universitat de València), Facultat de Física, Universitat de València, E-46100 Burjassot, València, Spain
(Received 26 July 1993)

Density functionals that reproduce the helium liquid-gas interface as a function of temperature have been used, within an improved homogeneous nucleation approach, to investigate thermal nucleation and cavitation in both helium isotopes. The results are compared with available experimental data on cavitation in ^{3}He and ^{4}He. Predictions are made for cavitation in ^{3}He at negative pressures and for nucleation in both isotopes.

I. INTRODUCTION

Superheated liquids and supercooled vapors are examples of metastable systems. Although they are internally stable, there exists in each case another configuration having a lower chemical potential. The metastable state is separated from the stable one by some thermodynamical barrier. Because of statistical fluctuations in density, that barrier can be overcome as a result of the formation and growth of bubbles in the liquid or droplets in the vapor (bubbles and droplets will be here generically referred to as clusters).

The study of nucleation-driven phase changes has attracted great interest for many years. Liquid helium is especially appealing for homogeneous nucleation studies, due to its particular features at low temperatures. Motivated by recent experimental work on cavitation in superfluid ^{4}He,[1] we have undertaken the study of thermal cavitation in both helium isotopes at high densities to investigate the formation of bubbles in the liquid, while at low densities, the reverse situation, i.e., drop formation in helium vapor, is considered.

The basic tool for this study is constituted by two density functionals, one for each isotope, which we have constructed to describe with some accuracy the equation of state, liquid-vapor equilibrium, and thermal properties of the interface.[2,3] These functionals allow one to obtain the nucleation (cavitation) barrier within an improved version of the homogeneous nucleation theory as indicated for example by Xiong and Maris[4] and by Oxtoby.[5]

In a previous work, we have used this method to investigate thermal cavitation in liquid helium at negative pressures.[6] The aim of the present work is to complete that study in two ways. First, presenting results on cavitation in helium at positive pressures, and second, studying the formation of drops in the vapor. We shall show that our results on cavitation at positive pressures are in agreement with the experimental data,[7,8] opposite to the situation for ^{4}He at negative pressures.[6] We are not aware of existing experimental results for nucleation in either helium isotope away from the critical point. The critical region is deliberately excluded from our calculations because of the intrinsic limitations of the density functionals we are using,[2,3] as well as the very low temperature region in which nucleation through quantum tunneling may play a significant role.[9] Notwithstanding, the present study almost spans the whole liquid-gas equilibrium region, making quite distinct predictions in physical situations where no experimental information is available.

II. THERMAL NUCLEATION WITHIN A DENSITY FUNCTIONAL APPROACH

The nucleation rate J, i.e., the number of drops or bubbles formed in the homogeneous system per unit time and volume, is given in the original Becker-Döring theory by the expression

$$J = J_0 \exp\left(-\Delta\Omega/kT\right), \tag{1}$$

where $\Delta\Omega$ is the difference between the grand canonical potential corresponding to the critical cluster and that of the homogeneous system, T is the temperature, and k the Boltzmann constant. The preexponential factor J_0 depends on the characteristics of the system and on the dynamics of the nucleation process.

Within the so-called classical theory of nucleation (see, for example, Refs. 5, 10, 11 and references therein), the grand potential of the growing drop is evaluated in the capillarity approximation. It consists in treating the drop as a piece of bulk liquid limited by a sharp surface. Such a macroscopic approximation has at least two obvious shortcomings. First, the neglect of any compressional effect on the central density of the drop due to its surface. This is what one calls a finite size effect, such as the change in energy of the cluster due to curvature corrections. These corrections can be incorporated as variations of the surface energy with size, leading to a kind of

droplet model for homogeneous nucleation.[12] The second shortcoming is originated by the inability of the model to take into account the modification in the surface energy of the cluster due to the presence of vapor as T increases.

These limitations, certainly important for small size clusters, can be overcome using a density functional to calculate the thermodynamical properties of the system,[4,6,10,13] and this indeed constitutes our starting point. As we have thoroughly discussed,[2,3] the free energy density of either helium isotope can be written as

$$f(\rho,T) = f_{\rm NI}(\rho,T) + \frac{1}{2}b\rho^2 + \frac{1}{2}c\rho^{2+\gamma} + \beta\frac{(\nabla\rho)^2}{\rho} + \xi(\nabla\rho)^2 \equiv f_{\rm vol}(\rho,T) + \beta\frac{(\nabla\rho)^2}{\rho} + \xi(\nabla\rho)^2 , \quad (2)$$

where ρ is the particle density and $f_{\rm NI}$ is the well-known free energy density of a noninteracting Bose or Fermi gas.[14] The density gradient terms vanish when the system is homogeneous, in which case $f(\rho,T)$ reduces to $f_{\rm vol}(\rho,T)$. The parameters b, c, γ, β, and ξ have been adjusted so as to reproduce physical quantities such as the surface tension, equation of state, and vapor pressure along the coexistence line. This is of special relevance for a quantitative study of homogeneous nucleation and cavitation in the liquid-gas transition.

Figure 1 shows a schematic picture of the phase equilibrium diagram in the pressure-density plane, which may represent either helium isotope.[15] The region below the dash-dotted line is the two-phase coexistence region. For a given T, the densities of the liquid and vapor in equilibrium are found imposing that the pressure and chemical potential of both phases be the same, i.e.,

$$\mu(\rho_L,T) = \mu(\rho_V,T), \quad (3)$$
$$P(\rho_L,T) = P(\rho_V,T),$$

with μ and P calculated from $f_{\rm vol}$. These equations have a nontrivial solution only for T below a critical value T_c. The two-phase equilibrium region splits into two domains. One is the unstable region in which the system cannot exist as a uniform phase. The other one is a metastable region where the system can remain homogeneous until a small perturbation drives it into a two-phase equilibrium state. These domains are separated by the classical spinodal curve defined as

$$\left(\frac{\partial P}{\partial \rho}\right)_T = 0. \quad (4)$$

The spinodal line is represented in Fig. 1 by the solid line labeled sp, and the metastability region corresponds to the hatched zone limited by the spinodal and the two-phase coexistence curves. Both curves are tangent at the critical point (P_c,T_c). Three generic isotherms are also drawn in that figure.

The liquid may be driven into a metastable state, for example, by superheating it at constant P (going from point 1 to point 2; see Fig. 1) or decreasing P at constant

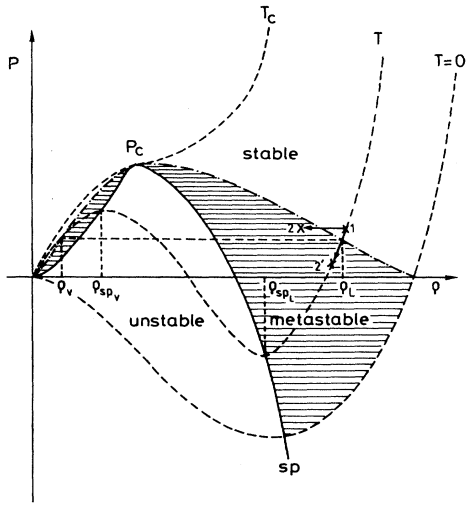

FIG. 1. Schematic representation of the liquid-gas equilibrium. The solid line labeled sp is the spinodal line, and the dash-dotted line is the two-phase equilibrium line. The regions of stability, metastability and unstability of the one-phase system are also indicated.

T (going from point 1 to point 2′). These processes cause the system to cross the liquid-gas equilibrium line, penetrating into the metastable zone. The dynamics of the first-order phase transition corresponding to liquid-gas separation can be regarded as the formation of clusters of a new phase in the homogeneous metastable medium (bubbles in the liquid or drops in the vapor); for sizes smaller than a critical one, these clusters shrink, but beyond a critical radius, they grow to trigger the phase separation.

The application of the density functional approach to the nucleation problem proceeds in two steps. One determines first the critical cluster size for given values of T and P, and second, the pressure at which the number of critical clusters formed per unit time and volume equals a conventional number, say, one per second and cubic centimeter, to indicate the onset of phase separation.

We have obtained the liquid-gas coexistence line and the spinodal line respective, by solving Eqs. (3) and (4). These calculations involve only algebraic equations, since only $f_{\rm vol}(\rho,T)$ comes into play. Next, at given $T < T_c$ we pick up a density ρ_m for which the system is in the metastable region. For example, at the intermediate T shown in Fig. 1, ρ_m will lie between $\rho_{\rm sp_L}$ and ρ_L (bubble formation) or between ρ_V and $\rho_{\rm sp_V}$ (drop formation). Then, the density profile of the critical cluster is obtained solving the Euler-Lagrange equation

$$\frac{\delta f}{\delta \rho} = \frac{\partial f}{\partial \rho} - \nabla\frac{\partial f}{\partial \nabla\rho} = \mu , \quad (5)$$

where μ is the chemical potential of the homogeneous metastable system at (ρ_m,T). The boundary conditions for the physical solution of Eq. (5) are $\rho'(0) = 0$ and $\rho(r \to \infty) = \rho_m$. The nucleation barrier $\Delta\Omega$ is finally obtained from the difference between the grand potential

of the critical cluster and of the homogeneous metastable system:

$$\Delta\Omega = \int d\mathbf{r}\,[f(\rho,T) - f_{\rm vol}(\rho_m,T) - \mu(\rho-\rho_m)]\,. \quad (6)$$

Since the pressure of the homogeneous system is $P = -f_{\rm vol}(\rho_m,T) + \mu\rho_m$, Eq. (6) yields $\Delta\Omega$ as a function of P and T.

In Fig. 2 we plot the nucleation barrier $\Delta\Omega$ as a function of P for both isotopes corresponding to bubble formation at positive pressures and different temperatures. As expected, for a given temperature, $\Delta\Omega$ drops to zero at the corresponding spinodal pressure, since at that point the homogeneous system becomes macroscopically unstable. It is worth mentioning[5,11] that a weak point of the classical theory is that it yields nonvanishing barriers at the spinodal line. At the opposite extreme, $\Delta\Omega$ diverges when P approaches the vapor pressure value. This simply indicates that, to have an appreciable probability of forming a bubble, the system has to be immersed deeply inside the two-phase equilibrium region, the probability for any of these critical clusters being given by the exponential factor $\exp(-\Delta\Omega/kT)$ in Eq. (1).

To make a quantitative statement about the formation

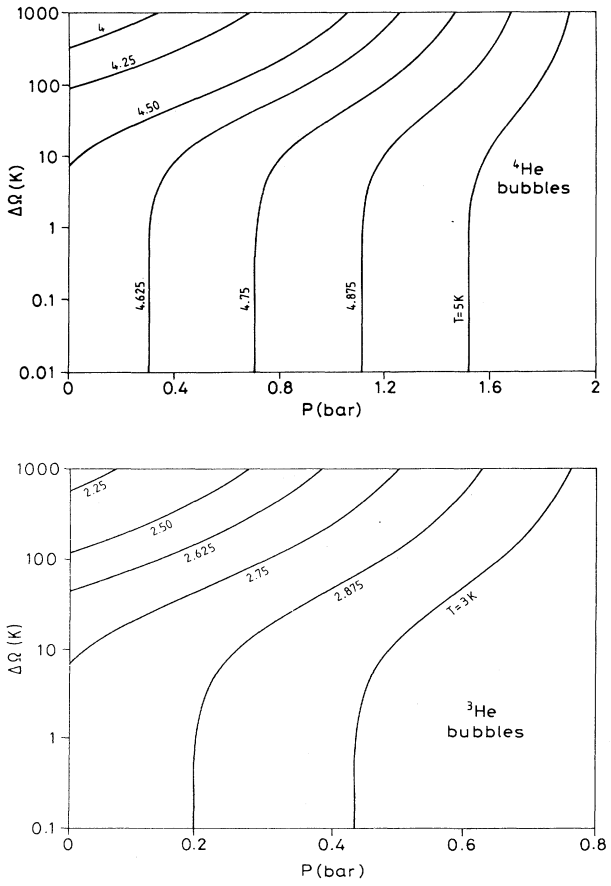

FIG. 2. Nucleation barriers as a function of pressure for ^{4}He (a) and ^{3}He (b) corresponding to bubble formation, at positive pressures.

of clusters in helium, let us define the pressure for homogeneous nucleation P_h at a given T, as that for which J equals one cluster per cubic centimeter per second:[7,10]

$$J_0 \exp(-\Delta\Omega/kT) = 1\ \text{cm}^{-3}\,\text{sec}^{-1}. \quad (7)$$

To solve Eq. (7) for P_h, an expression for the preexponential factor has to be chosen. There are many proposals of different complexity in the literature; see, for example, Refs. 4, 5, 7, and 8 and references therein. As in our previous work,[6] we have written the trial frequency per unit volume J_0 following Xiong and Maris, who take $J_0 = kT/(hV_{\rm cl})$, where $V_{\rm cl}$ is the volume of a sphere of radius 10 Å representing the critical cluster, and h is the Planck constant. To have an idea of the order of magnitude of this preexponential factor, for $T = 4$ K one has $J_0 \sim 2\times10^{31}$ cm^{-3} sec^{-1}, while for the same temperature Sinha *et al.*[7] have $J_0 \sim 2\times10^{33}$ cm^{-3} sec^{-1}. A variation of two orders of magnitude in J_0, which is also obtained when the preexponential factor is calculated by means of theories developed to describe the dynamics for the formation of critical clusters,[5] does not affect in any appreciable way the solution of Eq. (7), and so we are not going to discuss here the validity of the different prefactors in the literature.

To make a sensible comparison with the experimental results of Refs. 1 and 7, we have solved

$$J = (V\tau)_e^{-1}, \quad (8)$$

where the choice $(V\tau)_e = 2.5\times10^{-13}$ cm^{3}sec corresponds to solving the equation for the experimental conditions of the work of Xiong and Maris.[1] Taking $(V\tau)_e = 1$ cm^3 sec, Eq. (8) reduces to Eq. (7).

III. RESULTS

A. Cavitation

Figures 2–5 together with Figs. 1 and 2 of Ref. 6 collect the main results we have obtained on cavitation in both isotopes. As we have mentioned before, in Fig. 2 we have plotted the nucleation barriers for cavitation as a function of P for positive pressures. Note that each barrier has been obtained along an isotherm, and so these T curves cannot intercept each other. At high temperatures, the curves are almost vertical, since the spinodal ($\Delta\Omega = 0$) and the saturation ($\Delta\Omega \to \infty$) pressures are close. At low T the saturation pressure is ~ 0 and the spinodal one is about -9 bars for ^{4}He and -3 bars for ^{3}He,[6] and the T curves show a large kind of plateau (in a logarithmic scale); see Figs. 1 and 2 of Ref. 6.

If classical nucleation is applied, none of these T curves will cross the P axis. These barriers resemble ours for large values but abruptly separate for small ones, going asymptotically to zero when $P \to -\infty$.

The pressure of homogeneous bubble formation P_h is shown in Fig. 3 as a function of T for ^{4}He [Fig. 3(a)] and ^{3}He [Fig. 3(b)]. The solid curves have been obtained using $(V\tau)_e = 1$ cm^3 sec, and the dashed curves with $(V\tau)_e = 2.5\times10^{-13}$ cm^3 sec. It is worth noting that the

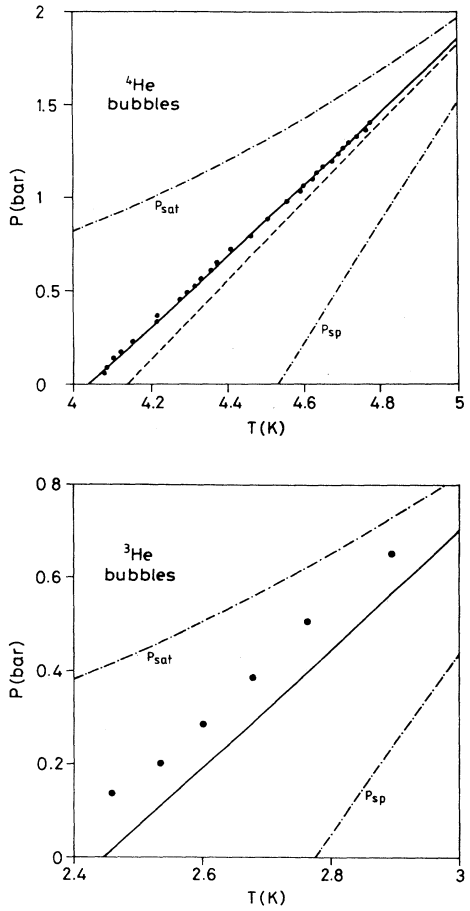

FIG. 3. Homogeneous cavitation pressure as a function of temperature for ^{4}He (a) and ^{3}He (b) at $P > 0$. The solid curves have been obtained using $(V\tau)_e = 1$ cm^3 sec, and the dashed ones using $(V\tau)_e = 2.5 \times 10^{-13}$ cm^3 sec. The experimental points are from Ref. 7 (^{4}He) and from Ref. 8 (^{3}He). The saturation vapor pressure line is indicated as $P_{\rm sat}$ and the spinodal line as $P_{\rm sp}$.

results of the calculation are rather insensitive to the precise value of $(V\tau)_e$ [compare the solid and dashed curves, whose $(V\tau)_e$ differ in 13 orders of magnitude].

In these figures we have also plotted the spinodal line $P_{\rm sp}$ and the vapor saturation curve $P_{\rm sat}$ as a function of T. The dots are experimental points taken from Ref. 7 for ^{4}He, and from Ref. 8 for ^{3}He. One can see that the agreement between theory and experiment is very good for ^{4}He, indicating that the density functional approach to homogeneous nucleation theory applies to bubble formation in ^{4}He at positive pressures. Concerning ^{3}He, the agreement is fairly good; our calculations are less than 0.1 K above the experimental results. This discrepancy could be attributed to a failure of the ^{3}He functional at such high temperatures (the ^{4}He one turns out to work much better; see Refs. 2 and 3), or to an experimental underestimation of the homogeneous nucleation temperature. This possibility is indicated, although ruled out, by Lezak *et al.*[8]

Comparing $P_{\rm sat}$ with P_h in Fig. 3, one can see, for example, that for ^{4}He at $T = 4.2$ K, the pressure has to be reduced from its value at saturation around 0.5 bar to get cavitation, while a reduction of 0.25 bar is enough at $T \sim 4.8$ K. For ^{3}He, the reduction at $T \sim 2.5$ K is around 0.35 bar, and ~ 0.1 bar at $T \sim 2.9$ K. An alternative way to read this figure is that, at $P = 1$ bar, one needs to increase T around 0.4 K to produce cavitation in ^{4}He, whereas an increase of ~ 0.1 K is necessary at $P = 1.5$ bars.

In Fig. 4 we show the pressures for homogeneous bubble formation from $T = 0$ to the vicinity of the critical point, which is indicated by a cross. The results below $T \leq 0.5$ K should be considered only as indicative, since we have neglected quantum tunneling.[9] As in Fig. 3, the solid line represents P_h for $(V\tau)_e = 1$ cm^3 sec and the dashed line, for $(V\tau)_e = 2.5 \times 10^{-13}$ cm^3 sec. Both curves merge with the spinodal line $P_{\rm sp}$ at $T = 0$. The influence of the precise value of $(V\tau)_e$ on P_h turns out to be more sizable for negative P_h, which happens for $T \leq 4$ K for ^{4}He and for $T \leq 2.4$ K in the case of ^{3}He (see Fig.

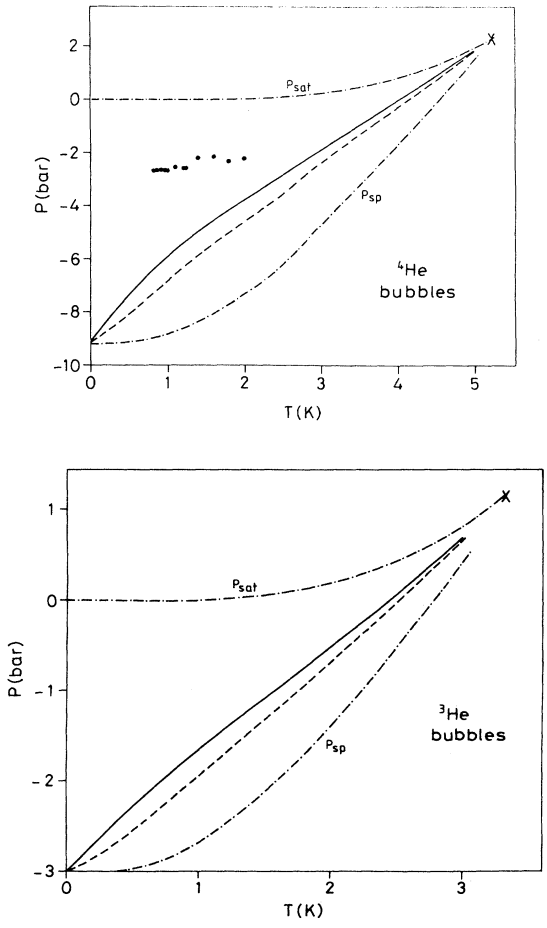

FIG. 4. Homogeneous cavitation pressure for ^{4}He (a) and ^{3}He (b) as a function of temperature. The lines have the same meaning as in Fig. 3. The dots in (a) are experimental points taken from Ref. 1.

3). The dots in Fig. 4(a) are the experimental points of Ref. 1. The possible origin of the discrepancy between the calculated P_h and the experimental results has been discussed in Refs. 1 and 6.

The present results show the interest of performing experiments on ^{4}He above the λ transition ($T_\lambda = 2.17$ K), but still for temperatures such that $P_h < 0$, i.e., $T \leq 4$ K. Indeed, at high temperatures the density functional approach yields results in good agreement with those obtained from the classical theory.[7] This can be easily understood if one realizes that at these temperatures the critical bubbles are large (see Fig. 5), so that finite size effects are less important. As T decreases, the critical bubbles get smaller and the classical theory becomes less reliable, whereas the density functional approach still applies. If this is the case, the remaining discrepancy between theory and experiment below T_λ could be attributed, on firmer grounds, to the role played by vortices in the process of cavitation in superfluid ^{4}He. Alternatively, the planned experiments on cavitation in ^{3}He (Ref. 1) could help understanding if the existing discrepancy for ^{4}He is still due to shortcomings of the density functional approach.

Figure 5 shows the density profile of several critical bubbles we have found in ^{4}He and ^{3}He. Their size grows as T increases due to the decrease of the surface tension. It is also interesting to observe the filling of the bubble with gas as T increases, and the appreciable increase of the surface diffuseness as it happens for the liquid surface at saturation.[2,3] The comparatively large value of asymptotic density for ^{4}He at $T = 2$ K reflects the experimental fact that the density of the liquid at saturation presents a maximum for $T \sim 2.2$ K.

B. Nucleation

Figures 6–8 show the results for nucleation in both isotopes. In Fig. 6 we have plotted the nucleation barrier as a function of pressure calculated along different isotherms. The range of temperatures goes from zero to almost the critical temperature. Similarly to what has been previously indicated for bubble formation, one can see that $\Delta\Omega$ drops to zero at the pressure corresponding to the spinodal line, and diverges when it approaches the saturation value.

The pressure P_h of homogeneous droplet nucleation is shown in Fig. 7 as a function of T. The meaning of the curves is the same as in Fig. 3. Note that the difference between P_h and $P_{\rm sat}$ is rather small, of the order of 0.1

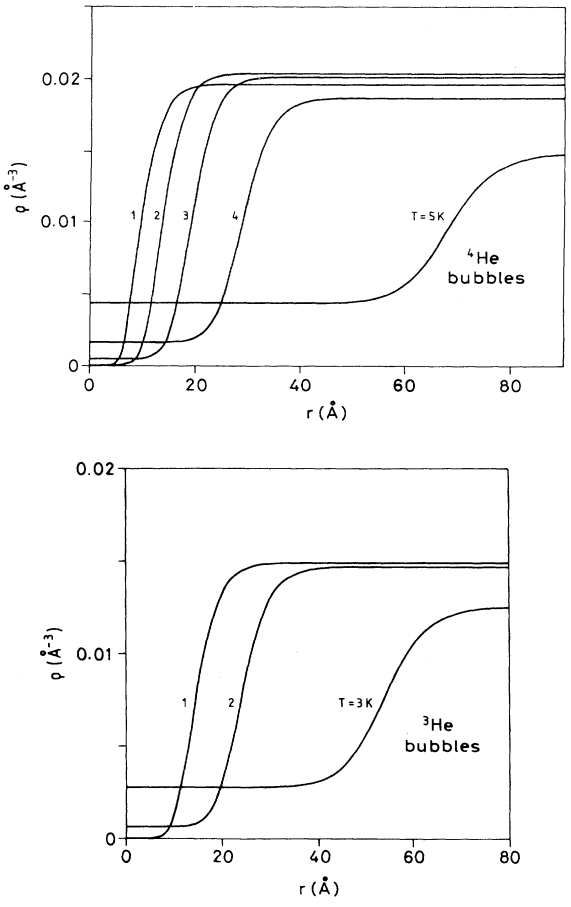

FIG. 5. Critical bubbles for ^{4}He (a) and ^{3}He (b) at the indicated temperatures.

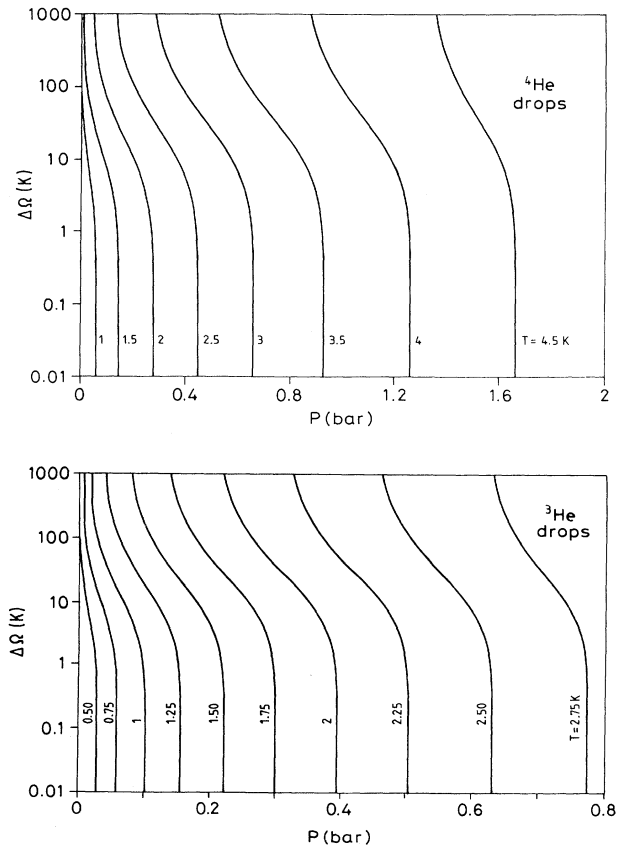

FIG. 6. Nucleation barriers as a function of pressure for ^{4}He (a) and ^{3}He (b) corresponding to drop formation.

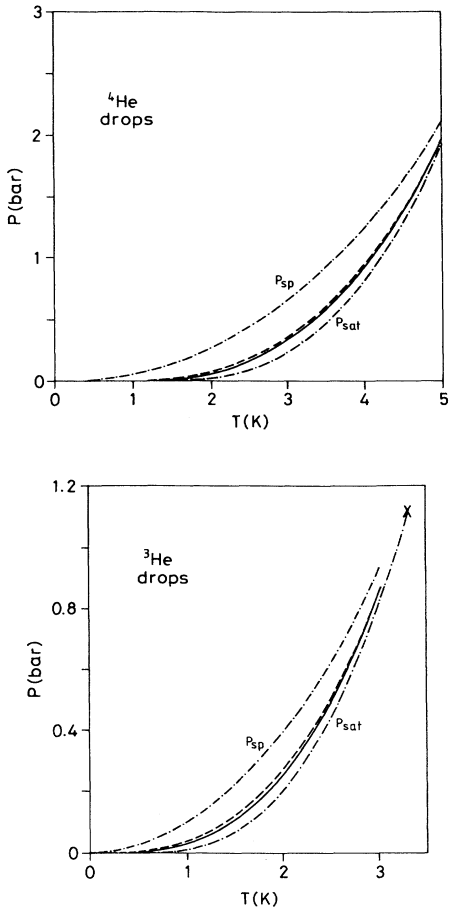

FIG. 7. Homogeneous nucleation pressure as a function of temperature for ^{4}He (a) and ^{3}He (b). The lines have the same meaning as in Fig. 3.

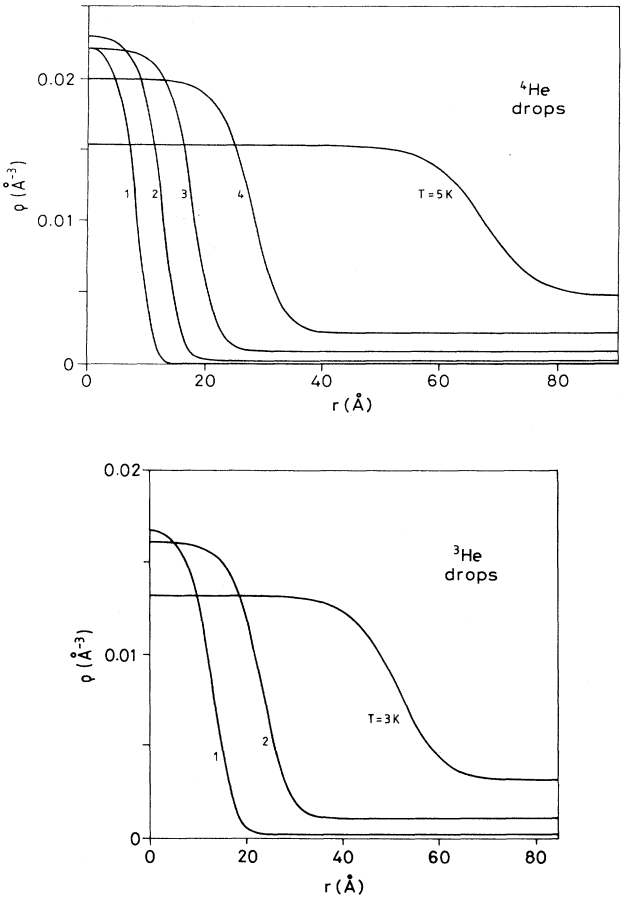

FIG. 8. Critical drops for ^{4}He (a) and ^{3}He (b) at the indicated temperatures.

bar for ^{4}He above $T \sim 2$ K, and ~ 0.03 bar for ^{3}He above $T \sim 1$ K. This indicates that experiments aiming at studying homogeneous nucleation in helium will be much harder to analyze in the gas than in the liquid phase. We would also like to draw the attention on the negligible influence of the value of $(V\tau)_e$ on P_h.

Finally, in Fig. 8 the density profiles of the critical droplets we have found are plotted, for temperatures ranging from $T = 1$ to 5 K in ^{4}He [Fig. 8(a)] and for $T = 1$, 2, and 3 K in ^{3}He [Fig. 8(b)]. Again one can see that, due to the decrease of the surface tension, the critical droplets grow as T increases. Comparing Figs. 5 and 8, one can see that for each isotope, at given T the sizes of the critical drop and bubble are similar (see also Ref. 10).

IV. DISCUSSION

We have thoroughly investigated the processes of thermal nucleation and cavitation in helium using density functionals that accurately reproduce the experimental liquid-gas equilibrium. Our calculations reproduce very well the experimental results on cavitation in ^{4}He at positive pressures, and fairly well those of ^{3}He in the same conditions.

At high temperatures, classical nucleation theory yields results similar to those we have obtained using a density functional (see Refs. 7 and 8). We coincide with Oxtoby (see Ref. 5 and references therein) that this agreement is basically due to the large size of the critical cluster, which justifies the use of the capillarity approximation. At low temperatures, the critical sizes are small and the approximation breaks down. This and the fact that when T decreases P_h is shifted from values relatively near $P_{\rm sat}$ to values much closer to $P_{\rm sp}$,[18] where the classical theory predicts nonzero barriers, preclude the applicability of the classical approach at low temperatures. A dramatic consequence of these drawbacks is that the classical P_h can be bigger in absolute value than $P_{\rm sp}$, as first pointed out in Ref. 1.

A large discrepancy still exists between the calculated pressure for homogeneous cavitation in superfluid ^{4}He and the experimental results of Ref. 1 (see also Refs. 6 and 16). To ascertain if this is due to heterogeneous cavitation on vortex lines,[1,17] experiments above T_λ and

below 4 K are called for. If, as we expect, these results smoothly joint the existing ones at $P > 0$, the difference between the experimental results of Xiong and Maris[1] and our calculations can be likely attributed to cavitation on vortex lines. It would be very interesting to have experimental results on ^{3}He available at negative pressures, since it is a normal quantum fluid above 2.7 mK. The possibility of having results from both isotopes will give a definite answer to the question of whether or not a density functional approach can be applied to homogeneous nucleation in a quantum fluid, for which one already knows that classical nucleation theory is unreliable at low temperatures.

A possible extension of the present work is to study nucleation in ^{3}He-^{4}He mixtures.[19] Work in this direction is now in progress.

ACKNOWLEDGMENTS

This work has been supported by DGICYT (Spain) Grant Nos. PB89-0332 and PB92-0820. D.M.J. thanks the CICYT (Spain), and M.G. the Departament d'Ensenyament of the Generalitat de Catalunya, for financial support. We thank the generous computer support of the CESCA facility.

* Permanent address: Departamento de Física, Facultad de Ciencias Exactas y Naturales, Universidad de Buenos Aires, RA-1428 Buenos Aires, Argentina.

[1] Q. Xiong and H.J. Maris, J. Low Temp. Phys. **82**, 105 (1991).
[2] M. Barranco, M. Pi, A. Polls, and X. Viñas, J. Low Temp. Phys. **80**, 77 (1990).
[3] A. Guirao, M. Centelles, M. Barranco, M. Pi, A. Polls, and X. Viñas, J. Phys. Condens. Matter **4**, 667 (1992).
[4] Q. Xiong and H.J. Maris, J. Low Temp. Phys. **77**, 347 (1989).
[5] D.W. Oxtoby, J. Phys. Condens. Matter **4**, 7627 (1992).
[6] M. Guilleumas, M. Pi, M. Barranco, J. Navarro, and M.A. Solís, Phys. Rev. B **47**, 9116 (1993).
[7] D.N. Sinha, J.S. Semura, and L.C. Brodie, Phys. Rev. A **26**, 1048 (1982).
[8] D. Lezak, L.C. Brodie, J.S. Semura, and E. Bodegom, Phys. Rev. B **37**, 150 (1988).
[9] I.M. Lifshitz and Yu. Kagan, Zh. Eksp. Teor. Fiz. **62**, 385 (1972) [Sov. Phys. JETP **35**, 206 (1972)].
[10] D.W. Oxtoby and R. Evans, J. Chem. Phys. **89**, 7521 (1988).
[11] D.W. Oxtoby, in *Fundaments of Inhomogeneous Fluids*, edited by D. Henderson (Marcel Dekker, New York, 1992), Chap. 10, p. 407.
[12] A. Dillmann and G.E.A. Meier, J. Chem. Phys. **94**, 3872 (1991).
[13] X.C. Zeng and D.W. Oxtoby, J. Chem. Phys. **94**, 4472 (1991).
[14] R. K. Pathria, *Statistical Mechanics* (Pergamon, Oxford, 1972).
[15] Strictly speaking, the T=0 isotherm in Fig. 1 corresponds to the ^{4}He case. For ^{3}He at low densities, one would have the pressure of the free Fermi gas; i.e., the pressure should increase even at zero temperature.
[16] J.A. Nissen, E. Bodegom, L.C. Brodie, and J.S. Semura, Phys. Rev. B **40**, 6617 (1989).
[17] F. Dalfovo, Phys. Rev. B **46**, 5482 (1992).
[18] This is easy to see if one realizes that at given T, P_h is the intersection of the corresponding T curve in Fig. 2, or in Fig. 1 of Ref. 6 for example, with the line $\Delta\Omega = kT \ln J_0$ obtained from Eq. (7), which is an increasing function of T.
[19] J.K. Hoffer and D.N. Sinha, Phys. Rev. A **33**, 1918 (1986).